Thermal Study of Hybrid Photovoltaic Thermal (PV-T) Solar Air Collector Using Finite Element Method

Naima Boulfaf*‡, Jamal Chaoufi*, Abdelaziz Ghafiri*, Abdallah Elorf*

*Laboratory of Electronics, Signal Processing and Modelling Physics, Department of Physics,
Ibn Zohr University, 80000 Agadir, Morocco.
(naimaboulfaf@gmail.com, jchaoufi@gmail.com, abdelaazizghafiri@gmail.com, elorf.abdel@gmail.com)

‡ Corresponding author; Naima Boulfaf, Ibn Zohr University, 80000 Agadir, Morocco, Tel.: +212693975608,
naimaboulfaf@gmail.com

Received: 01.12.2015 Accepted: 29.02.2016

Abstract- The hybrid photovoltaic thermal (PV-T) solar systems generate electricity and heat simultaneously. This type produce a higher energy conversion rate compared with a traditional solar collecting system and than conventional PV modules. The ambient air circulation is used as a simple mode for heat extraction. This study investigates the thermal performance of the PV-T solar air collector. The theoretical and numerical studies of PV-T air collector operating in dynamic mode had been performed. The basic equations of thermal balance were determined. The resolution of those equations is done using finite element method which the domain of study is discretized to triangular elements and nodes. A computer code has been developed for this calculation in order to carry the numerical simulation and a thermal model has been developed in this case study. The temperature profiles of glazing, solar cells, aluminum plate and outlet air have been determined. The influence of some parameters such as air mass flow rate, ambient temperature, solar radiation, the length of the collector and air velocity has also been carried out. The obtained results showed that the solar cells layer possessed the highest temperature whatever the value of solar intensity and ambient temperature. It's also shown that the PV-T length is an important geometrical parameter for the thermal efficiency of the collector. The air velocity effect on the PV-T collector is obvious when it increases from 0 to 1 m/s and higher wind speed causes the cooling of solar cells which cause the decrease in the temperature of the PV module.

Keywords- Photovoltaic thermal, Computer code, Finite element method, Dynamic mode, Temperature distribution.

1. Introduction

Most of the absorbed solar radiation by PV cells is not converted into electricity and increases their temperature which causing a decrease in their electrical efficiency. This undesirable effect can be partially avoided by a proper heat extraction with a natural or forced fluid circulation. In PV-T solar systems, the reduction of PV module temperature can be combined with useful fluid heating. Therefore, hybrid PV-T systems can simultaneously provide electrical and thermal energy, achieving a higher energy conversion rate of the absorbed solar radiation. These systems consist of PV modules coupled to heat extraction devices in which air or water of lower temperature than that of the PV modules is heated, while at the same time, the PV module temperature is reduced. In PV-T system applications, the production of electricity is the main priority, and therefore, it is necessary to operate the PV modules at low temperature in order to keep the solar cell electrical efficiency at a sufficient level. PV-T systems provide a higher energy output than standard PV modules and could be cost effective if the additional cost of the thermal unit is low. Several models of hybrid PV-T solar air heater had been proposed in the past.

Kern and Russed [1] are studied the main concepts of PV-T collector using water or air as the coolant. Hendrie [2] and Florschuetz [3] have included PV-T modeling in their works. Raghuraman [4] has developed numerical methods predicting PV-T collector performance. Cox and Raghuraman [5] have performed numerical simulations to optimize the design of flat plate PV-T solar air collector in order to increase the solar absorptance and reducing the infrared emittance. Bhargava et al [6] have analyzed a hybrid system which is a combination of an air heater and photovoltaic system parameters such as length of the collector and air mass flow rate. Garg and Adhikar [7] have proposed a numerical simulation model for predicting the thermal and electrical productivities of PV-T air collectors with simple and double glass configurations. Sofian et al [8] have proposed a new design of double pass PV-T collector which can produce more thermal energy, while simultaneously having a productive cooling effect on the PV cell.

Hagazy [9] has compared the thermal and electrical performance of four hybrid photovoltaic thermal solar air collectors which are differentiated by the cooling mode of PV modules. Kalogirou [10] has studied monthly performance of an unglazed hybrid PV-T system under forced mode of operation for climatic condition of Cyprus. Mei et al [11], Cartmel et al [12] have presented the dynamic model of a PV-T collector integrated in the facade of a building. Tiwari et al [13] have validated the theoretical and experimental results for PV module integrated with air duct for composite climate of India. They concluded that an overall thermal efficiency of the PV-T system has significantly increased (18%) due to utilization of thermal energy from PV module. Tiwari and sodha [14] have proposed parametric study of various configurations of hybrid PV-T air collector. These systems are differentiated by the presence or absence of glazing and tedlar. The results showed that glazed PV-T without tedlar gives the best performance.

Joshi and Tiwari [15] have evaluated the energy and exergy analysis of a hybrid PV-T air collector. The results experimentally validated indicate that energy and exergy efficiency of PV-T air heater varies between 55- 65 and 12-15%, respectively. Othman et al [16] have carried out the theoretical and experimental study of thermal and electrical productivity of a finned double-pass PV-T solar air collector. The results show that the use of fins increases both the thermal efficiency and electrical performance of the collector. Tripanagnostopoulos [17] has presented a new type of PV-T collector with dual heat extraction operation with aspects and improvements of PV-T solar energy systems. Zondag [18] has performed a rigorous review on research work of a PV-thermal collector and system, carried out by various scientists till 2006. His review includes history and importance of photovoltaic hybrid system and its application in various sectors. It also includes characteristics equations, study of design parameters and marketing, etc. Joshi et al. [19] have developed a thermal model for the PV module integrated with solar air collector and validated it experimentally. They have indicated that PV module temperature can be controlled and reduced in consequence of changing the mass flow rate of air in solar collector and the efficiency of PV module can be increased.

Chow [20] has done a review on PV-T hybrid solar technology especially PV-T air collector systems. His article gives a review of the trend of development of the technology, in particular the advancements in recent years and the future work required. Energy and exergy analysis of hybrid micro-channel photovoltaic thermal module has been carried by Agrawal and Tiwari [21] and they concluded that micro-channel photovoltaic thermal module gives better results. Kumar and Rosen Mark [22] have critically reviewed PV-T air collectors for air heating providing useful results relating to the practicability of these collectors for preheating air to suit a large variety of applications. Rajoria et al. [23] have performed overall thermal energy and exergy analysis of hybrid PV-T array considering four array configuration and concluded that the performance of case III is better than rest of the cases.

Agrawal et al. [24] have given the design and indoor experiment analysis of glazed hybrid photovoltaic thermal tiles air collector connected in series and concluded that if the numbers of glazed PV-T tile are connected in series then it will be more beneficial from overall energy and overall exergy point of view. Singh et al. [25] have performed comparative study of different types of hybrid photovoltaic thermal air collectors and reported that overall annual thermal energy, exergy gain and exergy efficiency of unglazed hybrid PV-T tiles air collector was improved by 32%, 55.9% and 53% respectively, over the conventional PV-T air collectors. Yang and Athienitis [26] presented a prototype open loop air-based building integrated photovoltaic thermal BIPVT system with a single inlet is studied through a comprehensive series of experiments in a full scale solar simulator recently built at Concordia University. Singh et al. [27] have developed a model for single channel unglazed PV-T module and optimized design parameter using Genetic Algorithms and concluded that the maximum overall exergy efficiency is 16.88% at optimized parameters.

In this paper, a PV-T solar air collector has been simulated and its performance over different operating conditions and parameters were studied. We have developed a detailed numerical model to search the temperature

distribution of the PV-T air collector. In most of works carried in the literature, the numerical approach that found is based on the electrical thermal analogy or on finite element software. In our study we have proposed a detailed systematic approach which allows moving from a boundary problem difficult to resolve in a more accessible and simplified problem. This approach consists in partitioning the domain (PV-T) in various layers independent of each other, each layer is discretized into small elements for each element we will search a simplified formulation of the problem. The built model has also the advantage of allowing adding or removing a layer. By varying these layers we can see the influence on the solar cells temperature and consequently on the thermal and electrical performance of PV-T air collector.

2. Presentation of physical model

In this part we resolute the transient heat transfer problem. Consider a homogeneous and anisotropic PV-T solar air collector with total thickness E, length L and width H. This collector consists of seven layers: glass, solar cells, EVA, aluminum plate, flowing fluid, insulating material and back aluminum plate. The temperature distribution in this collector is evaluated in two dimensions by the temperature function *T(x, y, t)*. Suppose then at time t = 0 the PV-T occupies the interval [0, L] of x-axis, and [0, E] of y- axis, the temperature distribution is known at any point *M(x, y)* of the domain, and equal to the ambient temperature $T_a = T_0(x, y)$. Suppose, also that the collector is submitted to a solar radiation $G = 1000w/m^2$ and the side faces at x = 0 and x = L are supposed insulated. Fig. 1 shows the cross-sectional view of a PV-T air collector.

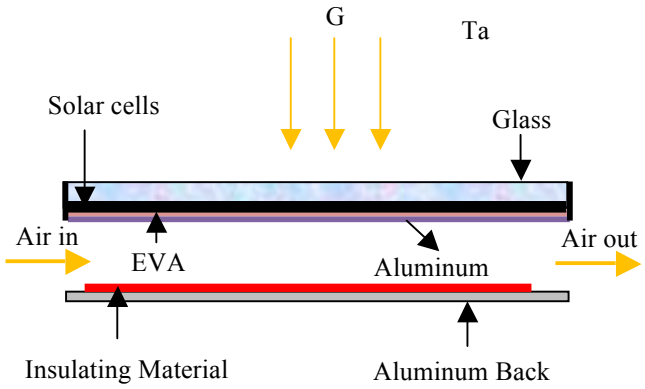

Fig. 1. The cross-sectional view of a PV-T air collector.

3. Theoretical analysis

In order to write the energy balance equation for each component of PV-T collector, the following assumptions have been made:

- The radiation is neglected.
- The thermo-physical parameters of different materials of PV-T are supposed to be independent on temperature.
- The notion of perfect contact is counted for adjacent elements.
- It is considered that the flowing fluid is a perfect incompressible gas.

ρ,c and the components of $\bar{\bar{\lambda}}$ are positive constants, representing respectively the density, specific heat and the components of thermal conductivity tensor. The determination of the temperature distribution of PV-T at point M of coordinates *(x, y)* at time t amounts to solving for each component the heat equation [28, 29]:

$$\rho c \frac{\partial T}{\partial t} = div\left(\bar{\bar{\lambda}}\, \overrightarrow{grad T}\right) \quad (1)$$

Where:

$$\left[\bar{\bar{\lambda}}\right] = \begin{bmatrix} \lambda_{11} & \lambda_{12} \\ \lambda_{21} & \lambda_{22} \end{bmatrix} \quad (2)$$

3.1. Equation of the problem

The determination of the temperature distribution in the PV-T collector amounts to solving equation system Eq. (1) associated with the boundary conditions of each component. The boundary conditions for each layer are:

- ***Glass***

The upper face of glass is subjected to solar radiation G and exchange heat by convection with the ambient air. The lower face L_{g2} is subjected to a flux transmitted from the face L_{g1}, the flux is null on the right L_{g3} and left face L_{g4}.

$$-\lambda_g \overrightarrow{grad T_g}.\vec{n} = \alpha_g G - h_{g-a}(T_g - T_a) \;\; on \;\; L_{g1} \quad (3a)$$

$$-\lambda_g \overrightarrow{grad T_g}.\vec{n} = \alpha_g \tau_g G \;\; on \;\; L_{g2} \quad (3b)$$

The flux is null on L_{g3} and L_{g4}

Initial conditions: $T_g(x, y, 0) = T_{g0}(x, y) = T_a$ (3c)

- ***Solar cells***

Photovoltaic cells receive the solar flux that passes through the glass. The solar radiations incident on the PV cells leads to generating electric current and electric power. The boundary conditions are:

$$-\lambda_c \overrightarrow{grad T_c}.\vec{n} = \alpha_c \tau_g G \;\; on \;\; L_{c1} \quad (4a)$$

The flux is null on L_{c3} and L_{c4}

At surface:

$$\varphi = \eta_{ref}\left[1 - \beta_0(T_c - T_{ref}) + \varpi ln G\right]G \quad (4b)$$

Initial conditions: $T_c(x, y, 0) = T_{c0}(x, y) = T_a$ (4c)

- ***EVA***

The PV cells are deposited on a layer of EVA. We suppose that the flux is null on L_{eva3} and L_{eva4}.

Initial conditions: $T_{eva}(x,y,0) = T_{eva0}(x,y) = T_a$ (5)

- ***Aluminum Plate***

An aluminum plate is positioned on the EVA layer. This plate isolates the upper layers of the flowing fluid. The heat exchange between the plate and the fluid is convection-type with h_{Al-f} is the convective heat transfer coefficient. T_{Al} and T_f represent the temperature at the interface aluminum-fluid on the plate and fluid respectively. The boundary conditions are:

$$-\lambda_{Al}\overrightarrow{grad}T_{Al}.\vec{n} = -h_{Al-f}(T_{Al} - T_f) \quad on \quad L_{Al2} \tag{6a}$$

The flux is null on L_{Al3} and L_{Al4}

Initial conditions: $T_{Al}(x,y,0) = T_{Al0}(x,y) = T_a$ (6b)

- ***Insulating material***

The insulation serves to limit the energy loss and to maintain the heat in the coolant. Consequently, we suppose that the flux is null on L_{i3} and L_{i4}.

Initial conditions: $T_i(x,y,0) = T_{i0}(x,y) = T_a$ (7)

- ***Back Aluminum plate***

A second aluminum plate is placed as last for separating the insulation from the outside. The boundary conditions are:

$$-\lambda_{Alb}\overrightarrow{grad}T_{Alb}.\vec{n} = -h_{Alb-a}(T_{Alb} - T_a)\ on\ L_{Alb2} \tag{8a}$$

The flux is null on L_{Alb3} and L_{Alb4}

Initial conditions:

$$T_{Alb}(x,y,0) = T_{Alb0}(x,y) = T_a \tag{8b}$$

- ***Flowing fluid***

The flowing fluid used in this work is air. The boundary conditions involving these phenomena can be written as:

We must solve the following equation:

$$\rho_f c_f \frac{\partial T_f}{\partial t} = div(\bar{\bar{\lambda}}_f \overrightarrow{grad}T_f) - \dot{m}c_f(T_f - T_{fin}) \tag{9a}$$

With boundary conditions:

$$-\lambda_f\overrightarrow{grad}T_f.\vec{n} = -h_{f-Al}(T_f - T_{Al}) \quad on\ L_{f1} \tag{9b}$$

Imposed temperature:

$$T_{fin} = T_a \ on\ L_{f3} \tag{9c}$$

The flux is null on L_{f2} and L_{f4}

Initial conditions: $T_f(x,y,0) = T_{f0}(x,y) = T_a$ (9d)

3.2. Variational formulation

To solve the problem, we can proceed by multiplying the heat conduction equation by a regular test function T^* and transform it into an integral form. The equivalent problem to solve is given by:

Finding the temperature *T (x, y, t)* such that:

- ***Glass***

$$W(T_g, T_g^*) = \int_S \rho_g c_g T_g^* \left(\frac{\partial T_g}{\partial t}\right) dS - \int_{L_2} T_g^*\, \alpha_g \tau_g G dL - \int_{L_1} T_g^* \left(\alpha_g G - h_{g-a}(T_g - T_a)\right) dL + \int_S \overrightarrow{grad}T_g^* (\bar{\bar{\lambda}}_g \overrightarrow{grad}T_g)\, dS = 0 \tag{10}$$

- ***Solar cells***

$$W(T_c, T_c^*) = \int_S \rho_c c_c T_c^* \left(\frac{\partial T_c}{\partial t}\right) dS - \int_{L_1} T_c^*\, (\alpha_c \tau_v G) dL + \int_S \overrightarrow{grad}T_c^* (\bar{\bar{\lambda}}_c \overrightarrow{grad}T_c)\, dS + \int_S T_c^* (\eta_{ref}\beta_0\, T_c G) dS - \int_S T_c^* \eta_{ref} G\left[1 + \beta_0 T_{ref} + \varpi lnG\right] dS = 0 \tag{11}$$

- ***EVA***

$$W(T_{eva}, T_{eva}^*) = \int_S \rho_{eva} c_{eva} T_{eva}^* \left(\frac{\partial T_{eva}}{\partial t}\right) dS + \int_S \overrightarrow{grad}T_{eva}^* (\bar{\bar{\lambda}}_{eva} \overrightarrow{grad}T_{eva})\, dS = 0 \tag{12}$$

- ***Aluminum Plate***

$$W(T_{Al}, T_{Al}^*) = \int_S \rho_{Al} c_{Al} T_{Al}^* \left(\frac{\partial T_{Al}}{\partial t}\right) dS + \int_{L_2} T_{Al}^* \left(h_{Al-f}(T_{Al} - T_f)\right) dL + \int_S \overrightarrow{grad}T_{Al}^* (\bar{\bar{\lambda}}_{Al} \overrightarrow{grad}T_{Al})\, dS = 0 \tag{13}$$

- ***Flowing fluid***

$$W(T_f, T_f^*) = \int_S \rho_f c_f T_f^* \left(\frac{\partial T_f}{\partial t}\right) dS + \int_{L_1} T_f^* \, h_{f-Al}(T_f - T_{Al}) dL + \int_S \dot{m} c_f T_f^* (T_f - T_{fin}) dS + \int_S \overrightarrow{grad} T_f^* (\bar{\bar{\lambda}}_f \overrightarrow{grad} T_f) \, dS = 0 \quad (14)$$

- ***Insulating material***

$$W(T_i, T_i^*) = \int_S \rho_i c_i T_i^* \left(\frac{\partial T_i}{\partial t}\right) dS + \int_S \overrightarrow{grad} T_i^* (\bar{\bar{\lambda}}_i \overrightarrow{grad} T_i) \, dS = 0 \quad (15)$$

- ***Back Aluminum plate***

$$W(T_{Alb}, T_{Alb}^*) = \int_S \rho_{Alb} c_{Alb} T_{Alb}^* \left(\frac{\partial T_{Alb}}{\partial t}\right) dS + \int_{L_2} T_{Alb}^* \left(h_{Alb-a}(T_{Alb} - T_a)\right) dL + \int_S \overrightarrow{grad} T_{Alb}^* (\bar{\bar{\lambda}}_{Alb} \overrightarrow{grad} T_{Alb}) \, dS = 0 \quad (16)$$

3.3. Solving the problem using the finite element method

3.3.1. Finite element technique

The objective of the finite element method is to find the temperature field T (x, y, t) at any point (x, y) at each time t. We will demonstrate how the problem is reduced to an ordinary differential system in t. To do this, precede to the discretization of the domain Ω in N_e sub domains Ω_e named elements. The geometry of these elements is three-node triangular. The number of nodes at each layer is n = 9 and the number of elements is n_t = 8 then at the overall structure (PV-T collector) the total number of nodes is N = 45 and the total number of elements is Nt = 56. Fig. 2 shows the PV-thermal discretization.

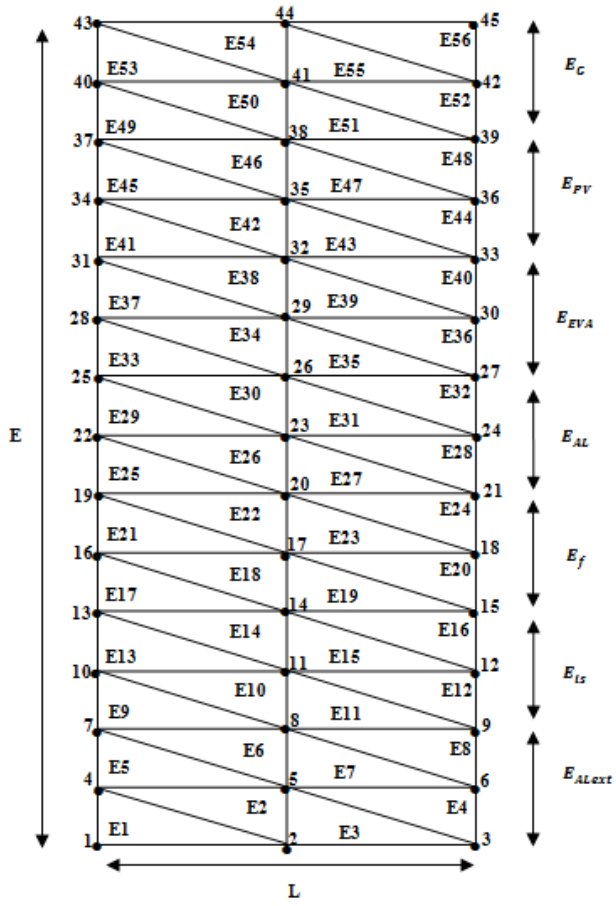

Fig. 2. Schematic of PV-thermal discretization using triangular elements.

3.3.2. Elementary representation of the temperature field

The approximate solution searched is the temperature function [30]:

$$T^e(x, y, t) = \sum_{i=1}^{3} T_i^e(t) N_i^e(x, y) \quad (17)$$

Such as the functions of interpolations:

$$N_i^e(x_i, y_j) = \delta_{ij} = \begin{cases} 1 & if \quad j = i \\ 0 & other \; wise \end{cases} \quad (18)$$

We can write the previous equality in matrix form:

$$T^e(x, y, t) = [N^e]\{T^e\} \quad (19)$$

Similarly for the function test:

$$T^{*e}(x, y, t) = [N^e]\{T^{*e}\} \quad (20)$$

The components $T_i^e(t)$ of the temperature vector $\{T^e\}$ are interpreted as approximate numerical value of $T(x, y, t)$ at the nodes. After calculations and simplifications we get:

$$W(T^e, T^{*e}) = \{T^{*e}\}^T \left([c^e]\{\dot{T}^e\} + [k^e]\{T^e\} - \{f^e\}\right) \quad (21)$$

Where $[c^e]$, $[k^e]$ and $\{f^e\}$ are respectively the element capacity matrix, the element conductance matrix and the element load vector.

The element capacity matrix, element conductance matrix and element load vector of each layer are given by:

- ***Glass***

$$[c_g^e] = \rho_g c_g \int_{S^e} [N^e]^T [N^e]\, dS^e \tag{22a}$$

$$[k_g^e] = \int_{S^e} [B^e]^T [\lambda_g] [B^e] dS^e + \int_{L_1^e} [N^e]^T h_{g-a} [N^e] dL^e \tag{22b}$$

$$\{f_g^e\} = \int_{L_1^e} [N^e]^T (\alpha_g G + h_{g-a} T_a) dL^e + \int_{L_2^e} [N^e]^T \alpha_g \tau_g G dL^e \tag{22c}$$

- ***Solar cells***

$$[c_c^e] = \rho_c c_c \int_{S^e} [N^e]^T [N^e] dS^e \tag{23a}$$

$$[k_c^e] = \int_{S^e} [B^e]^T [\lambda_c] [B^e] dS^e + G\eta_{ref}\beta_0 \int_{S^e} [N^e]^T [N^e] dS^e \tag{23b}$$

$$\{f_c^e\} = \eta_{ref} G [1 + \beta_0 T_{ref} + \varpi ln G] \int_{S^e} [N^e]^T dS^e + \alpha_c \tau_c G \int_{L_1^e} [N^e]^T dL^e \tag{23c}$$

- ***EVA***

$$[c_{eva}^e] = \rho_{eva} c_{eva} \int_{S^e} [N^e]^T [N^e] dS^e \tag{24a}$$

$$[k_{eva}^e] = \int_{S^e} [B^e]^T [\lambda_{eva}] [B^e] dS^e \tag{24b}$$

$$\{f_{eva}^e\} = 0 \tag{24c}$$

- ***Aluminum plate***

$$[c_{Al}^e] = \rho_{Al} c_{Al} \int_{S^e} [N^e]^T [N^e] dS^e \tag{25a}$$

$$[k_{Al}^e] = \int_{S^e} [B^e]^T [\lambda_{Al}] [B^e] dS^e + \int_{L_2^e} [N^e]^T h_{Al-f} [N^e] dL^e \tag{25b}$$

$$\{f_{Al}^e\} = 0 \tag{25c}$$

- ***Flowing fluid***

$$[c_f^e] = \rho_f c_f \int_{S^e} [N^e]^T [N^e] dS^e \tag{26a}$$

$$[k_f^e] = \int_{S^e} [B^e]^T [\lambda_f] [B^e] dS^e + \int_{L_1^e} [N^e]^T h_{f-Al} [N^e] dL^e + \dot{m} c_f \int_{S^e} [N^e]^T [N^e]\, dS^e \tag{26b}$$

$$\{f_f^e\} = \left[\dot{m} c_f \int_{S^e} [N^e]^T [N^e] dS^e\right] \{T_{fin}^e\} \tag{26c}$$

- ***Insulating material***

$$[c_i^e] = \rho_i c_i \int_{S^e} [N^e]^T [N^e] dS^e \tag{27a}$$

$$[k_i^e] = \int_{S^e} [B^e]^T [\lambda_i] [B^e] dS^e \tag{27b}$$

$$\{f_i^e\} = 0 \tag{27c}$$

- ***Back aluminum plate***

$$[c_{Alb}^e] = \rho_{Alb} c_{Alb} \int_{S^e} [N^e]^T [N^e] dS^e \tag{28a}$$

$$[k_{Alb}^e] = \int_{S^e} [B^e]^T [\lambda_{Alb}] [B^e] dS^e + \int_{L_2^e} [N^e]^T h_{Alb-a} [N^e] dL^e \tag{28b}$$

$$\{f_{Alb}^e\} = h_{Alb-a} T_a \int_{L_2^e} [N^e]^T dL^e \tag{28c}$$

3.3.3. Global representation and Assembly

a. Assembly at the layer

The ordinary differential system obtained in the element is written as:

$$\{T^{*e}\}^T \left([c^e] \left\{ \frac{\partial T^e}{\partial t} \right\} + [k^e]\{T^e\} \right) = \{T^{*e}\}^T \{f^e\} \quad (29)$$

$[A^e]$ is the matrix for passing from temperature vectors $\{T\}$ and temperature test vector $\{T^*\}$ to vectors $\{T^e\}$ and $\{T^{*e}\}$.

Firstly we have:

$$\{T^e\} = [A^e]\{T_{layer}\} \quad (30)$$

And

$$\{T^{*e}\} = [A^e]\{T^*{}_{layer}\} \quad (31)$$

Secondly, since the entire domain Ω can be partitioned into disjoint sub domains Ω^e :

$$\Omega = \bigcup_{e=1}^{e=n_t} \Omega^e \quad (32)$$

Finally, through the assembly of the elementary quantities, we can write the system obtained from the spatial discretization in matrix:

$$[c_{layer}]\{\dot{T}_{layer}\} + [k_{layer}]\{T_{layer}\} = \{f_{layer}\} \quad (33)$$

The matrix c, k and the vector f are given by:

$$[c_{layer}] = \sum_{e=1}^{e=n_t} ([A^e]^T [c^e][A^e]) \quad (34a)$$

$$[k_{layer}] = \sum_{e=1}^{e=n_t} ([A^e]^T [k^e][A^e]) \quad (34b)$$

$$\{f_{layer}\} = \sum_{e=1}^{e=n_t} [A^e]^T \{f^e\} \quad (34c)$$

b. Assembly at the overall structure (PV-T collector)

The global system to resolve is:

$$[\boldsymbol{C}]\{\dot{\boldsymbol{T}}\} + [\boldsymbol{K}]\{\boldsymbol{T}\} = \{\boldsymbol{F}\} \quad (35)$$

$[P]$ is the matrix for passing from the layer to overall structure.

The global matrix C, K and the vector F are given by:

$$[C] = \sum_{layer=1}^{7} [P]^T [c_{layer}]\ [P] \quad (36a)$$

$$[K] = \sum_{layer=1}^{7} [P]^T [k_{layer}]\ [P] \quad (36b)$$

$$\{F\} = \sum_{layer=1}^{7} [P]^T \{f_{layer}\} \quad (36c)$$

The resolution of a transient conduction problem allowed to resolute the first order differential system Eq. (35) in relation to time t.

With the initial conditions: $\{T_0\} = \begin{Bmatrix} T_1(0) \\ T_2(0) \\ \vdots \\ T_N(0) \end{Bmatrix}$ (37)

The determination of the temperature field in the material returns to determinate the temperature values in the nodes in time. The numerical resolution of the previous system allows determining the evolution of the temperature in the material for the known thermo-physical parameters.

c. Numerical solution of the problem

The integration of Eq. (35) is made by the matrix solution method.

Posing: $A = [C]^{-1}[K]$ and $B = [C]^{-1}\{F\}$ (38)

Searching the eigenvalues λ_i and eigenvectors

$$P = (v_1\ v_2\ v_3\ \ldots\ldots v_n) \quad (39)$$

Then calculate:

$$b_i' = P^{-1}B \quad (40)$$

And

$$A_i^0 = P^{-1}T(0) - \frac{b_i'}{\lambda_i} \quad (41)$$

Then we obtain:

$$X_i(t) = \frac{b_i'}{\lambda_i} + A_i^0 e^{-\lambda_i t} \quad (42)$$

The final expression can be written as:

$$T_i(t) = PX_i(t) \quad (43)$$

The design parameters and heat transfer coefficient of the photovoltaic-thermal air collector used in the present study are given in Table 1.

Table 1. Design parameters for photovoltaic thermal (PV-T) air collector.

Parameters	Values
E_G	0.006 m
E_C	0.0002 m
E_{EVA}	0.0005 m
E_{AL}	0.006 m
E_{IS}	0.05 m
E_F	0.03 m
E_{Alb}	0.003 m
L	1.026 m
H	0.528 m
λ_C	149 W/m °C
λ_G	1.2 W/m °C
λ_{EVA}	0.23 W/m °C
λ_{AL}	237 W/m °C
λ_F	0.02624 W/m °C
λ_{IS}	0.04 W/m °C
ρ_G	2500 kg/m^3
ρ_C	2330 kg/m^3
ρ_{EVA}	934 kg/m^3
ρ_{AL}	2698.9 kg/m^3
ρ_F	1.177 kg/m^3
ρ_{IS}	18 kg/m^3
C_G	840 J/kg
C_C	700 J/kg
C_{EVA}	57.5 J/kg
C_{AL}	897 J/kg
C_F	1005 J/kg
C_{IS}	1450 J/kg
α_G	0.05
α_C	0.9
τ_G	0.9
η_{ref}	0.125
β_0	0.0044
h	5.7 + 3.8 V

4. Results and discussion

The outlet air temperature, absorber and solar cells temperature have been evaluated by using Eq. (43) and the Matlab program for the given design and climatic parameters (Table 1). The results obtained are reported in Fig. 3-10.

Fig.3 shows the temperature variation of solar cells, EVA, aluminum plate, glass flowing fluid, insulating material and back aluminum with solar intensity Fig.3a and ambient temperature Fig.3b. It is evident that the solar cells temperature is higher than the other elements temperature whatever the value of solar intensity and ambient temperature.

The effect of mass flow rate on the variation of components temperatures is shown in Fig.4. It can be seen more the air flow is low more the components temperature is higher.

Fig.5 gives variation of temperatures with collector length. The components temperature increases with increasing length as expected. The PV-T length is therefore an important geometrical parameter for the thermal efficiency of the collector.

The evolution of the components temperature with air velocity is shown in Fig.6. It is evident from the figure that the increase in the air speed causes a decrease in temperature of the collector elements. In fact, the wind causes the cooling of solar cells which cause the decrease in the temperature of the PV module.

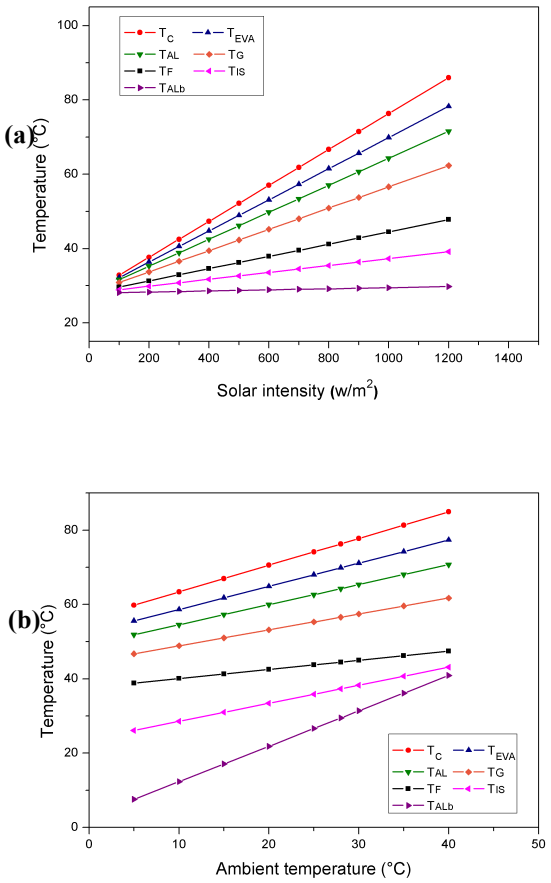

Fig. 3. (a) Variation of various temperatures with solar intensity, ($T_a = 28°C$ and $\dot{m} = 0.05Kg/s$). (b) Variation of various temperatures with ambient temperature, ($G = 1000W/m^2$ and $\dot{m} = 0.05Kg/s$).

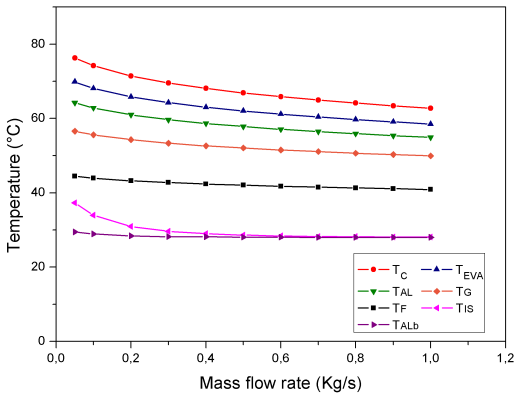

Fig. 4. Variation of various temperatures with mass flow rate, ($G = 1000W/m^2$ and $T_a = 28°C$).

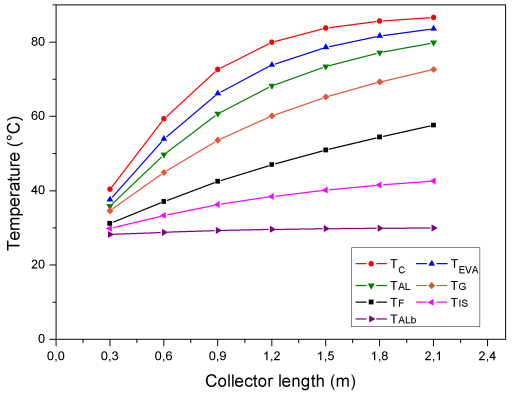

Fig. 5. Variation of various temperatures with collector length, ($G = 1000W/m^2$, $T_a = 28°C$ and $\dot{m} = 0.05Kg/s$).

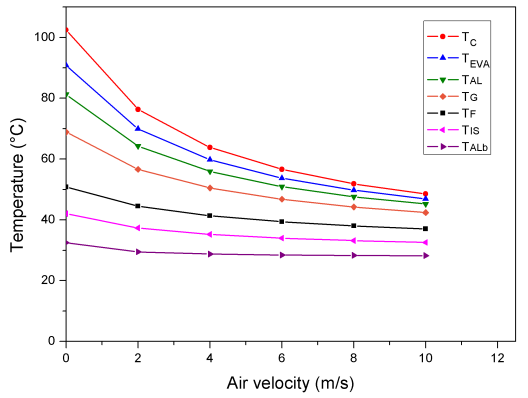

Fig. 6. Variation of various temperatures with air velocity, ($G = 1000W/m^2$ and $T_a = 28°C$).

Fig. 7 shows the hourly variation of various temperatures with time. It can be observed that the PV cells temperature is higher because they have a higher absorptivity relative to other elements. It can be seen that all elements of the collector have reached the steady state after a few hours.

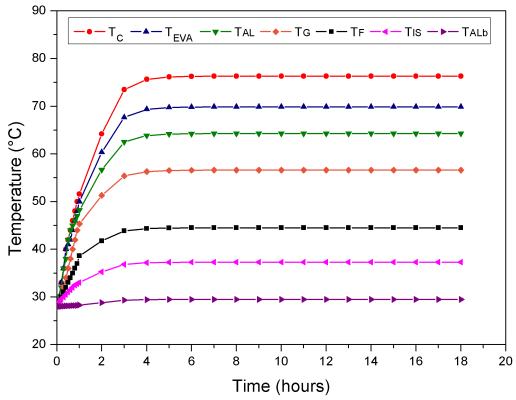

Fig. 7. Hourly variation of various temperatures with time, ($G = 1000W/m^2$, $T_a = 28°C$ and $\dot{m} = 0.05Kg/s$).

A parametric study was performed on the outlet air temperature and PV cells by varying the mass flow rate, the incident solar intensity, ambient temperature and time. The outlet air fluid temperature and PV cells decreases with mass flow rate (Fig. 10a and Fig. 10b) and its value increases with solar radiation (Fig. 8a and Fig. 8b) and ambient temperature (Fig. 9 and Fig. 9b) over time the temperature of the outlet air and PV cells increased in the first hours after it attains the steady state.

(a)

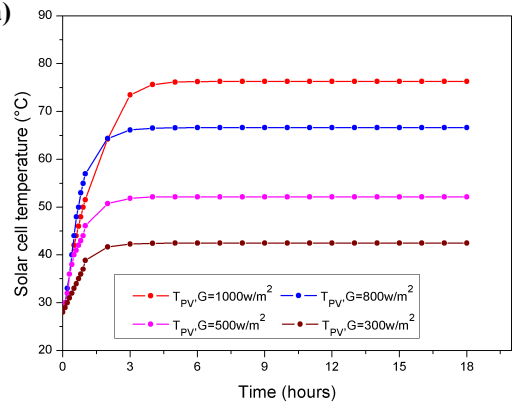

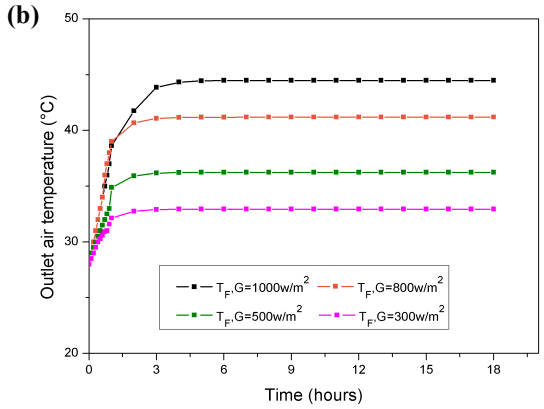

Fig. 8. (a) Hourly variation of solar cells temperature with different solar radiation. (b) Hourly variation of outlet air temperature with different solar radiation. ($T_a = 28°C$ and $\dot{m} = 0.05Kg/s$).

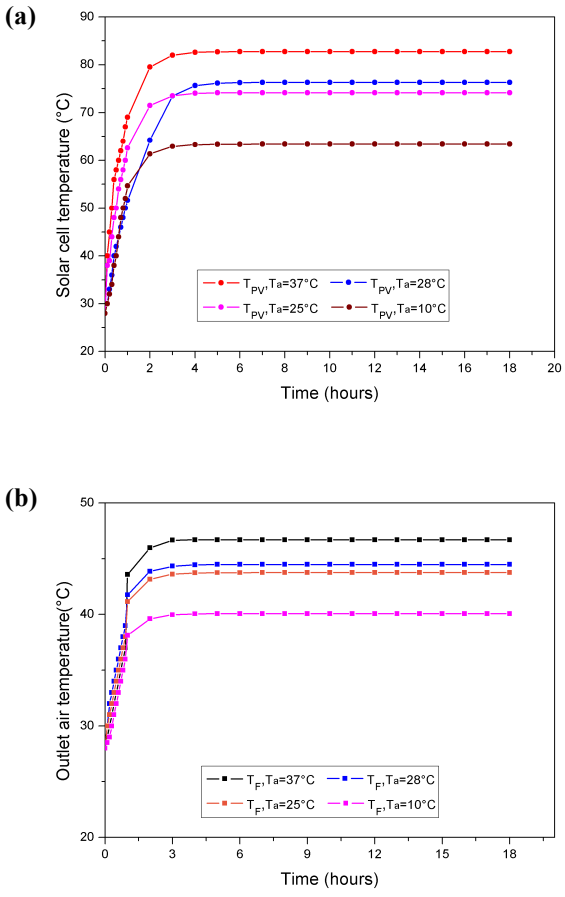

Fig. 9. (a) Hourly variation of solar cells temperature with different ambient temperature. (b) Hourly variation of outlet air temperature with different ambient temperature. ($G = 1000W/m^2$ and $\dot{m} = 0.05Kg/s$).

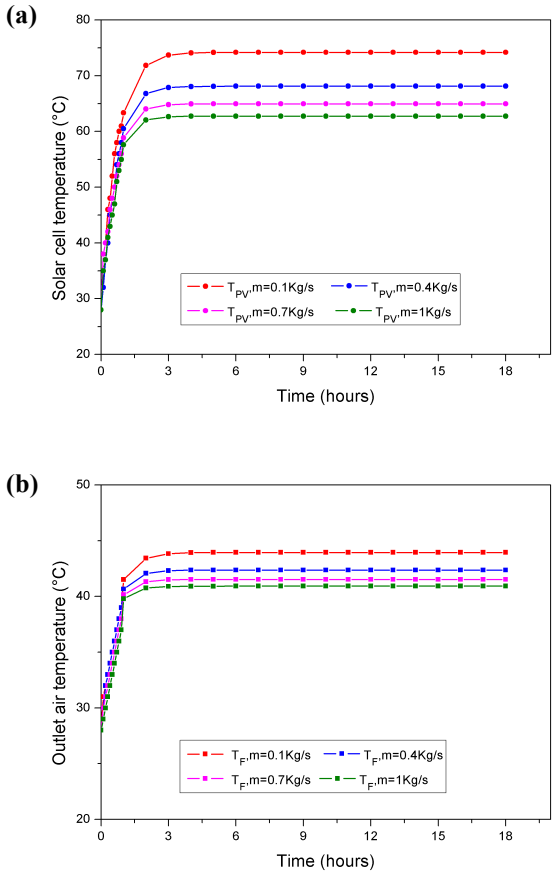

Fig. 10. (a) Hourly variation of solar cells temperature with different mass flow. (b) Hourly variation of outlet air temperature with different mass flow. ($G = 1000W/m^2$ and $T_a = 28°C$).

5. Conclusion

In this paper, the performance evaluation of PV-T air collector was carried out. A new and detailed thermal model based on finite element method was developed to calculate the thermal parameters of a typical PV-T air collector. A numerical simulations and parametric studies were performed. On the basis of present study, the following conclusions have been drawn:

- Increasing the solar radiation intensity or ambient temperature, the solar cells temperature increases.
- The components temperature increases with increasing length of the collector. The PV-T length is therefore an important geometrical parameter for the thermal efficiency of the collector.
- When the mass flow rate increase, the components temperature of a PV-T air collector decrease.
- The temperature of the collector elements decrease when the wind speed is increasing.
- The outlet air fluid and PV cells temperatures decreases with mass flow rate and its value increases with solar

radiation and ambient temperature. Lower ambient temperature is important for heat dissipation and the improving of solar cell electrical efficiency.

References

[1] Kern Jr EC, Russell MC, "Combined photovoltaic and thermal hybrid collector systems". In: Proc. 13th IEEE photovoltaic specialists, Washington (DC, USA); 1978. p. 1153–7.

[2] Hendrie SD, "Evaluation of combined photovoltaic/thermal collectors". In: Proceedings of international conference ISES, Atlanta, Georgia, USA, May 28– June 1, vol. 3. 1979. p. 1865–9.

[3] Florschuetz LW, "Extention of the Hottel–Whillier model to the analysis of combined photovoltaic/thermal flat plate collectors". Sol Energy 1979; 22:361–6.

[4] Raghuraman P, "Analytical predictions of liquid and air photovoltaic/thermal, flat-plate collector performance". J Sol Energy Eng 1981; 103:291–8.

[5] Cox III CH, Raghuraman P, "Design considerations for flat-plate photovoltaic/thermal Collectors". Sol Energy 1985; 35:227–41.

[6] Bhargava AK, Garg HP, Agarwall RK, "Study of a hybrid solar system-solar air heater combined with solar cells". Energy Convers Manage 1991; 31(5):471–9.

[7] Garg HP, Adhikari RS, "Conventional hybrid photovoltaic/thermal (PV/T) air heating collectors: steady-state simulation". Renew Energy 1997; 11: 363–85.

[8] Sopian K, Liu HT, Kakac S, Veziroglu TN, "Performance of a double pass photovoltaic thermal solar collector suitable for solar drying systems". Energy Convers Manage 2000; 41(4):353–65.

[9] Hegazy AA, "Comparative study of the performances of four photovoltaic/thermal solar air collectors". Energy Convers Manage 2000; 41:861–81.

[10] Kalogirou SA, "Use of TRYNSYS for modeling and simulation of a hybrid PV thermal solar system for Cyprus". Renew Energy 2001; 23:247–60.

[11] Mei, L.Infield, D.Eicker, U.et al., "Thermal modeling of a building with an integrated ventilated PV façade". Energy and buildings, Vol. 35, PP 605- 617, 2003.

[12] Cartmell, B.P. Shankland, N.J. Fiala, D et al., "A multioperational ventilated photovoltaic and solar air collector: application, simulation and initial monitoring feedback". Solar Energy, vol.76, pp 45-53, 2004.

[13] Tiwari A, Sodha MS, Chandra A, Joshi JC, "Performance evaluation of photovoltaic thermal solar air collector for composite climate of India". Sol Energy Mater Sol C 2006; 90(2):175–89.

[14] Tiwari A., Sodha M. S, "Parametric study of various configurations of hybrid PV/thermal air collector: Experimental validation of theoretical model". Solar Energy material and solar cells, 2006, Vol. 91 n°1 PP 17 – 28.

[15] Josi A. S., Tiwari A, "Energy and exergy efficiencies of a hybrid photovoltaic-thermal (PV/T) air collector". Renewable energy, 2007, Vol 32 n° 13, PP 2223-2241.

[16] Othman M. Y., Yatim B. Sopian K, "Performance study on a finned double pass photovoltaic-thermal (PV-T) solar collector". Desalination, 2007, Vol 209, n°1-3, PP 43- 49.

[17] Tripanagnostopoulos Y, "Aspects and improvements of hybrid photovoltaic/ thermal solar energy systems". Sol energy 2007; 81:1117–31.

[18] Zondag HA, "Flat-plate PV–thermal collectors and systems: a review". Renew Sustain Energy Rev 2008; 12(4):891–959.

[19] Joshi AS, Tiwari A, Tiwari GN, Dincer I, Reddy BV, "Performance evaluation of a hybrid photovoltaic thermal (PV/T) (glass-to-glass) system". Int J Therm Sci 2009; 48:154–64.

[20] Chow TT, "A review on photovoltaic/thermal hybrid solar technology". Appl Energy 2010; 87:365–79.

[21] S. Agrawal, G. N. Tiwari, "Energy and exergy analysis of hybrid micro-channel photovoltaic thermal module", Solar Energy, 85, 2011, pp 356-370.

[22] Kumar, Rakesh. Rosen Mark, A, "A critical review of photovoltaic– thermal solar collectors for air heating". Appl. Energy 2011; 88:3603–3614.

[23] Rajoria, C.S., Agrawal, S., Tiwari, G.N, "Overall thermal energy and exergy analysis of hybrid photovoltaic thermal array". Sol. Energy 2012; 86:1531–1538.

[24] Agrawal, S., Tiwari, G.N., Pandey, H.D, "Indoor experimental analysis of glazed hybrid photovoltaic thermal tiles air collector connected in series". Energy Build 2012; 53:145– 151.

[25] Singh, G.K., Agrawal, S., Tiwari, G.N, "Analysis of different types of hybrid photovoltaic thermal air

collectors: a comparative study". J. Fundamentals Renew. Energy Appl 2012.

[26] Yang, T., Athienitis, A.K, "A study of design options for a building integrated photovoltaic/thermal (BIPV/T) system with glazed and air collector multiple inlets". Sol. Energy 2014; 104:82–92.

[27] Singh, S., Agrwal, S., Tiwari, Arvind, Al-Helal, I.M., Avasthi, D.V, "Modeling and parameter optimization of hybrid single channel photovoltaic thermal module using genetic algorithms". Sol. Energy 2015; 113:78–87.

[28] Gouri Dhatt, Gilbert Touzot. A presentation of the finite element method. Collection University of compiegne, Maloine S.A. Publisher, 1981.

[29] Gouri Dhatt, Jean-Louis Batoz. Modeling of structures by finite element. Hermes 1990; vol 1 elastic solids.

[30] Gouri Dhatt, Gilbert Touzot, Emmanuel Lefrançois. Finite element method. Hermes Science, 2005.

Nomenclature

E	thickness (m)
S	area (m^2)
L	length of collector (m)
H	width of collector (m)
G	incident solar intensity ($W/m^{2)}$
C	specific heat (J/kg °C)
h	convective heat transfer coefficient (W/m^2 °C)
$\dot{m}$	mass flow rate (kg/s)
T	temperature (°C)
N_t	number of elements
N	number of nodes
Ω_e	sub domain
Ω	domain
L_1	upper face
L_2	lower face
L_3	right face
L_4	lift face
N_i	shape functions
[C]	thermal capacity matrix
[K]	thermal conductivity matrix
[F]	load vector
[B]	Derivative matrix
[A]	passage matrix
W	residual

Subscripts

a	ambient
c	solar cell
i	insulation
f	fluid
ref	reference
e	elementary
f_{in}	inlet fluid
Al	aluminum
b	back

Greek symbols

τ	transmitivity
α	absorptivity
ρ	density ($kg/m^{3)}$
λ	thermal conductivity (W/m °C)
β	packing factor of solar cell
η_{ref}	efficiency at standard test condition

Abbreviations

PV	photovoltaic
PV-T	photovoltaic-thermal
EVA	ethyl vinyl acrelate